

Specific Features of the Concentration Dependence of the Effective Mass, Electron Mobility and Oscillatory Phase of Magnetoresistivity in Non-Centrosymmetric Weyl Semimetal Candidate HgSe

S.B. Bobin, A.T. Lonchakov, V.V. Deryushkin, V.N. Neverov

*M.N. Miheev Institute of Metal Physics of Ural Branch of Russian Academy of Sciences,
620108, Yekaterinburg, Russia*

Abstract

In this paper, the authors report the results of an experimental study of effective mass, electron mobility and phase shift of Shubnikov de Haas oscillations of transverse magnetoresistance in an extended electron concentration region from $8.8 \times 10^{15} \text{ cm}^{-3}$ to $4.3 \times 10^{18} \text{ cm}^{-3}$ in single crystals of mercury selenide. The revealed features confirm the existence of a Weyl semimetal phase in HgSe at low electron density, which has been indicated by previous magnetotransport studies. However, the most significant result is the discovery of an abrupt change of Berry phase $\approx \pi$ at electron concentration $\approx 2 \times 10^{18} \text{ cm}^{-3}$, which we explain in terms of a manifestation of topological Lifshitz transition in HgSe that occurs by tuning Fermi energy via doping.

The increasing interest in Weyl semimetals (WSMs) in recent years has not only been in terms of fundamental research but also with respect to their potential for future engineering applications [1,2]. A WSM is a three-dimensional (3D) topological phase protected by a crystal symmetry and characterised by linear dispersion around pairs of nodes having opposite chirality. These so-called Weyl nodes are separated in momentum space; their only connection is through the sample boundary by exotic non-closed surface states known as Fermi arcs [3]. The present paper further develops a pioneering study [4] in which we reported spectacular transport properties in a HgSe sample with low ($2.5 \times 10^{16} \text{ cm}^{-3}$ at $T = 4.2\text{K}$) electron concentration, including strong non-saturating transverse magnetoresistance (MR), negative longitudinal MR, which is due to a chiral anomaly, and unusual for gapless semiconductors maxima of the temperature dependence of electrical resistivity. These features indicate the possibility of the coexistence of a WSM phase with a trivial gapless semiconductor phase in this material with zinc-blend structure. There are other experimental (ARPES investigation [5]) and theoretical [6, 7] justifications for proposing mercury selenide, a material with strong spin-orbit coupling, as a possible candidate in non-centrosymmetric WSMs. Mercury selenide is of significant interest for topological condensed matter physics as it presumably has four Weyl node pairs of the same type in bulk and surface topological Fermi arcs [6, 7]. This material can be considered as a simpler or “ideal” non-centrosymmetric WSM, the study of which is important for elucidating the exotic transport

properties that other non-centrosymmetric WSMs with a more complex Fermi surface topology exhibit [1]. The aim of this brief report is to provide evidence for the manifestation of a WSM phase in HgSe based on the concentration dependence of effective mass, Hall mobility and the Berry phase, which is a principal topological parameter of WSM kinetics.

Mercury selenide single crystals were grown using the Bridgman technique. Samples under investigation were cut from the homogeneous part of the single crystal ingots perpendicular to the direction of growth. Electron concentration in the range of $(10^{16} \lesssim n_e < 10^{18}) \text{ cm}^{-3}$ was obtained by varying the annealing time of the samples in Se vapour from ≈ 24 to ≈ 600 hours at temperatures of $(150 - 200)^\circ\text{C}$ [8]. Samples with $n_e \approx (1 - 5) \times 10^{18} \text{ cm}^{-3}$ were as-grown. In order to increase n_e above $2 \times 10^{18} \text{ cm}^{-3}$, samples were doped with donor impurities Ga or Fe [10]. All samples had the shape of a rectangular parallelepiped whose dimensions varied between $\approx (3.5 \times 1 \times 0.7) \text{ mm}^3$ and $\approx (8 \times 2 \times 1) \text{ mm}^3$ and which were not specifically oriented. The procedure of etching and electrical contact preparation is described in [4].

The effective mass $m_e(n_e)$ of the electrons in HgSe in the range of low $n_e < 1 \times 10^{17} \text{ cm}^{-3}$ attracted our interest due to a lack of experimental data in the literature. This particular region is especially relevant to a study of the topological properties of HgSe [4] since, in condensed matter physics, Weyl fermions are low-energy excitations. The cyclotron effective mass m_e of the electrons was deduced from the ratio of amplitudes of Shubnikov de Haas (SdH) oscillations of transverse MR $\rho_{xx}(B)$ measured at different temperatures. A detailed description of the method of obtaining m_e from the analysis of the SdH oscillations is given in [4]. SdH oscillations were extracted from $\rho_{xx}(B)$ after subtracting a smooth MR background. Magnetoresistance was measured using the standard four-probe method at temperatures 2, 4.2, 10 and 20K in a magnetic field up to 12T. The oscillatory component of transverse MR for several HgSe samples is shown in Fig.1. The insets demonstrate the fitting result of the ratio of oscillation amplitudes versus $1/B$ based on Lifshitz-Kosevich (LK) formula which yields the cyclotron effective mass [4].

Fig. 2 demonstrates our findings for the electron mass ratio m_e/m_0 as a function of n_e as well as the data for m_e/m_0 from [11,12], where m_0 is a free electron mass. It can be seen that, within the margin of error, effective mass does not depend on electron concentration in the range of $n_e \lesssim 1 \times 10^{17} \text{ cm}^{-3}$ down to the lowest concentration for our samples $\approx 9 \times 10^{15} \text{ cm}^{-3}$. On the one hand, this important result is not consistent with the generally accepted view of the non-parabolicity of the isotropic band Γ_8 in HgSe [13]. On the other hand, it can be interpreted as a confirmation of hypothesis [4] for the predominance of a topological semimetal phase in HgSe kinetics at low n_e because a rather long annealing time could lead to a depopulation of the conductivity band Γ_8 . It can be assumed that the Weyl fermion dispersion relation $\varepsilon(k)$ is not an

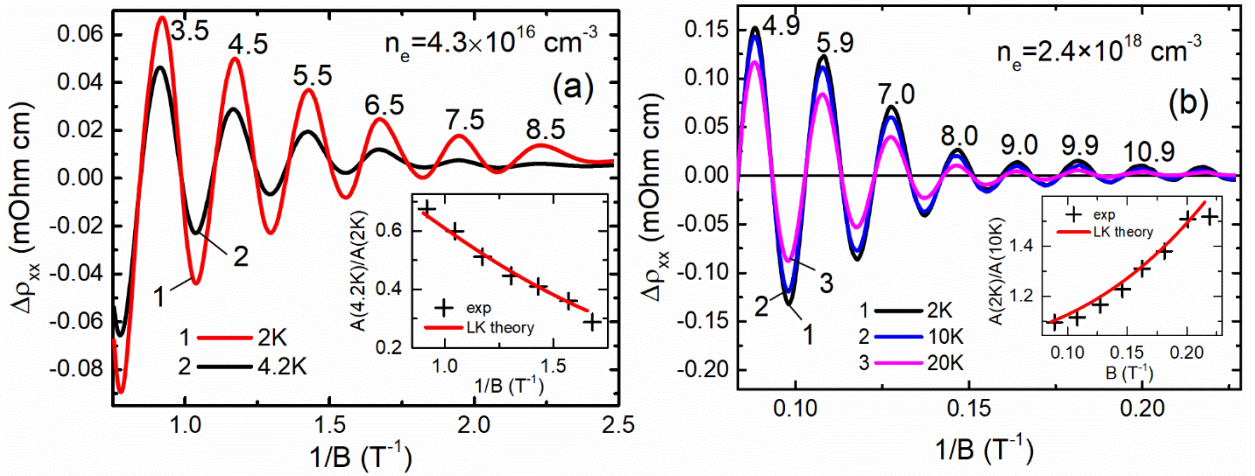


Fig. 1. The oscillatory component $\Delta\rho_{xx}$ of the transverse MR as a function of $1/B$ after subtracting the background of $\rho_{xx}(B)$ at different temperatures for the HgSe sample with $n_e = 4.3 \times 10^{16} \text{ cm}^{-3}$ (a) and $2.4 \times 10^{18} \text{ cm}^{-3}$ (b). The insets show the dependence of the oscillation amplitude ratio versus $1/B$ for the studied temperatures (symbols). The solid line is the fit to the LK formula used to determine the effective mass [4]. The parameter F/B_N is indicated for the maxima of $\Delta\rho_{xx}(1/B)$. This is half-integer for case (a) [Berry phase in non-trivial] and integer for case (b) [Berry phase close to zero] according to (5).

ideal Dirac-like dispersion, which generally deviates from the ideal Dirac cone, but can be described as in [14,15]:

$$\varepsilon(k) = \varepsilon_W + v_F \hbar k + \frac{\hbar^2 k^2}{2m_e}, \quad (1)$$

where ε_W is the energy at the Dirac point k_W , and v_F is the velocity at the Dirac point. As a result of (1), we detect nondependent on k electron effective mass at low n_e . Only at $n_e \gtrsim 5 \times 10^{17} \text{ cm}^{-3}$ can the dependence $m_e(n_e)$ be satisfactorily described using Kane's [16] non-parabolic isotropic dispersion law (solid line in Fig. 2). To fit the dependence $m_e(n_e)$ in two-band approximation (see formula (15) in [11]), we used the following parameters: $\varepsilon_g = \varepsilon(\Gamma_6) - \varepsilon(\Gamma_8) = -0.23 \text{ eV}$, which is the energy gap between light hole band Γ_6 and conduction band Γ_8 for trivial HgSe band structure, and $P = 7.7 \times 10^{-8} \text{ eV cm}$ which is the interband momentum matrix element. Thus, we can assume that, at a sufficiently large n_e , the concentration dependence of the effective mass points to the dominance of a trivial gapless semiconductor phase (conduction band Γ_8).

Unlike the effective mass, which is a parameter of the band spectrum, the mobility $\mu = e\tau_{tr}/m_e$ additionally characterises the electron scattering processes through the transport relaxation time τ_{tr} . We experimentally determined electron mobility using formula for Hall mobility $\mu_H = \sigma_0/n_e e$, where σ_0 is zero-field conductivity, e is the absolute value of the electron charge. In order to determine concentration n_e , we used the FFT frequency of SdH oscillations.

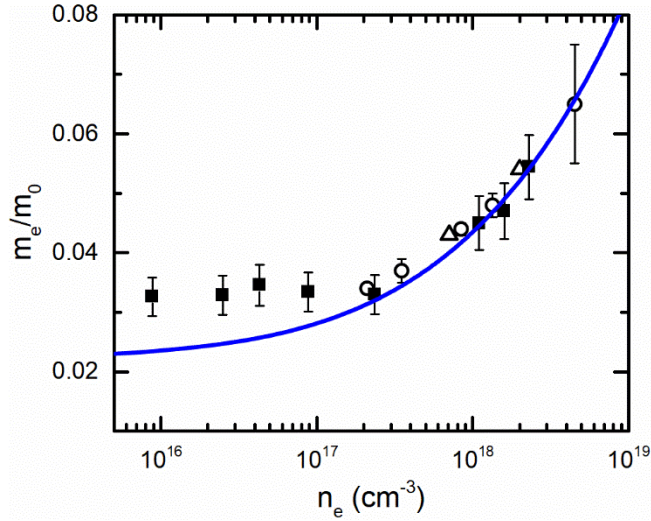


Fig. 2. Cyclotron effective mass in HgSe normalised to m_0 as a function of electron concentration at 4.2K. Filled squares – this work, open circles are from [11], open triangles are from [12], the solid line is the calculated effective mass for non-parabolic isotropic dispersion in two-band approximation.

Fig. 3 shows the concentration dependence of μ_H at $T = 4.2\text{K}$, consisting of the data of [9, 11, 17-19] combined with our own findings. After analysing this data, we distinguished three regions of $\mu_H(n_e)$ (Fig. 3). Region I corresponds to $n_e > n_{LT} \sim 10^{18} \text{ cm}^{-3}$, where n_{LT} is the concentration of the Lifshitz transition (LT), the discovery of which in HgSe is discussed below. Electron topological LT [20] is the abrupt topological change in the connectivity of the Fermi surface of material, giving rise to anomalies of its physical properties. With regard to the WSMs, bulk LT should be considered as a recombination of two non-trivial Fermi surfaces enclosing one Weyl node into a single trivial Fermi surface that encloses both Weyl nodes of opposite chirality [21-23]. This means that chirality is not well-defined, i.e. the total Berry flux through the Fermi surface equals zero. In Region I, the dependence $\mu_H(n_e)$ seem to be reasonably well described by the theory of ionised donor scattering (solid line on Fig. 3 from [18]) and transport properties should be determined by the trivial conduction band Γ_8 as mentioned above. Region II is limited to concentration interval of $10^{17} \lesssim n_e \lesssim 10^{18} \text{ cm}^{-3}$ below LT. This region is characterised with well-defined chirality, i.e. the formation of a separate Fermi surface for each Weyl node. It enables the additional mechanism of momentum relaxation – intervalley scattering or backscattering [23, 24], thereby leading to a deviation of the mobility from the theoretical value for ionised donor scattering (Fig. 3). However, with reduced n_e the corresponding decrease in τ_{tr} is accompanied by a decrease in m_e (Fig. 2). As a result, μ_H depends weakly on n_e in Region II. This region should be considered as a crossover of Region I and Region III ($n_c < n_e \lesssim 10^{17} \text{ cm}^{-3}$). In Region III, the transport and other properties of HgSe are fully determined by the topological semimetal phase. For example,

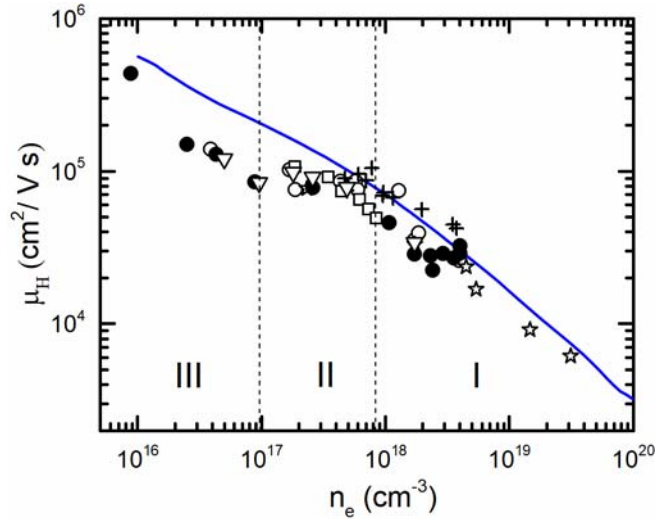


Fig. 3. Electron mobility in HgSe as a function of electron concentration at 4.2K. Filled circles – this work, open circles [9], crosses [17], open squares [11], stars [18], triangles [19]. The solid line is the calculated mobility for single-ionised-donor-scattering mode from [18]. Vertical dashed lines are drawn to separate three regions: Region I – the trivial gapless phase; Region III – the Weyl semimetal phase; Region II – crossover (for details see text).

in all samples from Region III, we observed negative longitudinal MR induced by chiral anomaly and non-trivial manifestation of topological properties in terms of the Hall effect which we will report in future papers. In Region III, m_e does not depend on n_e (Fig. 2). The decrease in n_e with a decrease in concentration of intrinsic donor-type defects in this region should lead to a decrease in the probability of backscattering and therefore to a strong increase in mobility. As seen in Fig. 3 the mobility reaches 4.3×10^5 cm 2 /V s at $n_e \approx 9 \times 10^{15}$ cm $^{-3}$, which is a record value for HgSe and higher than that of a TaAs when the Fermi level is located near the Weyl node W1 [23]. For the foregoing reasons, the above-mentioned concentration n_c formally corresponds to a boundary, below which the effective mass should tend to zero – as was observed, for example, in graphene when approaching the Dirac point [25]. It is reasonable to assume that reaching n_c in HgSe is unlikely due to the high defect density in this material.

A distinguishing feature of the Dirac quasiparticle is the nontrivial Berry phase of π associated with its cyclotron motion [26, 27]:

$$\Phi_B = \oint_{\Gamma} \vec{\Omega} \cdot d\vec{k}, \quad (2)$$

where Γ is the closed electron orbit [the intersection of the constant-energy surface, $\varepsilon(k) = \text{const}$, with the plane, $k_z = \text{const}$, where z is the direction of the magnetic field \vec{B}], and $\vec{\Omega}(\vec{k}) = i \int d\vec{k} u_{\vec{k}}^*(\vec{r}) \vec{\nabla}_{\vec{k}} u_{\vec{k}}(\vec{r})$ is the Berry connection; and $u_{\vec{k}}(\vec{r})$ is the amplitude of the Bloch wave

function. When the Berry phase is nonzero, the Onsager semiclassical quantisation rule [28] becomes [26]:

$$A_N \frac{\hbar}{eB} = 2\pi \left(N + \frac{1}{2} - \frac{\Phi_B}{2\pi} \right). \quad (3)$$

Here A_N is the extremal cross-sectional area of the Fermi surface related to the Landau level index N , \hbar is the Plank constant ($\hbar = h/2\pi$).

A straightforward way to detect the Berry phase in systems with a non-trivial topology is to study SdH oscillations since the basis of this phenomenon consists in a quantisation of orbital motion. Experimentally, a non-trivial π Berry phase was obtained from the analysis of SdH oscillations in topological insulators [15, 29-31], Dirac [32, 33] and Weyl [34] semimetals, as well as in graphene [25].

Let us briefly discuss the procedure of extracting the Berry phase from SdH oscillations of transverse MR. The first step is to consider the Fourier series of the transverse oscillatory component $\Delta\sigma_{xx}$ of the conductivity tensor [35]. For our purposes, it is sufficient to restrict ourselves to the first term of the Fourier expansion. This leads to the relation

$$\Delta\sigma_{xx} \sim -\cos 2\pi(F/B - \delta), \quad (4)$$

where $F = (A_N \hbar / 2\pi e)$ is a frequency of oscillations, $2\pi\delta$ is an additional phase shift with $\delta = 0$ for 2D and $\pm 1/8$ for 3D Fermi surfaces [34, 36, 37] and the minus before the cosine arises due to the first expansion coefficient in the Fourier series [35]. Next, it should be taken into account that in a strong magnetic field ($\omega_C \tau_{tr} \gg 1$, where $\omega_C = eB/m_e$ is the cyclotron frequency) $\Delta\sigma_{xx} \sim \Delta\rho_{xx}$ in the lowest order approximation for the small parameter $(\omega_C \tau_{tr})^{-1}$ [35, 38]. This means that the maximum of $\Delta\rho_{xx}(B)$ corresponds to that of $\Delta\sigma_{xx}(B)$ in a strong magnetic field. Thus, after replacing F/B in (4) by the Onsager relation (3) and accounting for the negative sign of cosine for the oscillation maximum of MR when the N th Landau level (LL) is crossing the Fermi energy one can obtain

$$\Delta\rho_{xx} \sim \cos 2\pi(N - \beta), \quad (5)$$

where $\beta = (\frac{\Phi_B}{2\pi} + \delta)$. It follows from (5) that, within the phase shift δ , the resistivity maximum $\Delta\rho_{xx}$ will correspond to the integer parameter F/B_N for the zero Berry phase and to the half-integer for the π -Berry phase. This leads to the widely employed procedure of determining the Berry phase: plotting the value of $1/B_N$ that corresponds to the N th maximum of $\Delta\rho_{xx}$ versus the integer LL index N in accordance with (3) (LL fan diagram of the SdH oscillations). Additionally, the minima of $\Delta\rho_{xx}$ with half-integer indexes N can be used for plotting LL diagrams [39]. The next step is to fit $1/B_N$ versus N dependence with a straight line and extract the intercept with N -axes. This intercept yields the value of phase shift β . The values of β between $-\frac{1}{8}$ and $+\frac{1}{8}$ indicate

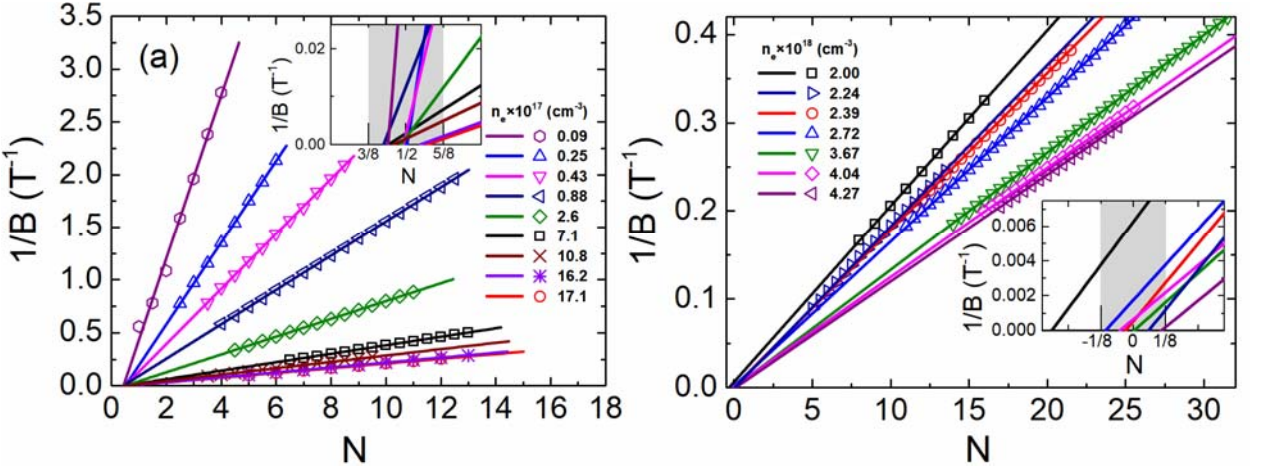


Fig. 4. Landau-level fan diagram for oscillations $\Delta\rho_{xx}(B)$ measured at $T=4.2\text{K}$ for HgSe samples with $n_e < n_{LT}$ (a) and $n_e \gtrsim n_{LT}$ (b), where n_{LT} is the critical concentration of the LT. The insets show a magnified view around the intercept. The intercept β is either between $3/8$ and $5/8$ for non-trivial Berry phase [grey area in the inset of panel (a)] or between $-1/8$ and $1/8$ for trivial Berry phase [grey area in the inset of panel (b)]. The only exception is $\beta \approx 0.2$ for the sample with concentration $n_e = 2 \times 10^{18} \text{ cm}^{-3}$ which we consider to be a critical concentration of the LT.

a trivial Berry phase and values of β between $\frac{3}{8}$ and $\frac{5}{8}$ indicate a non-trivial π - Berry phase. LL fan diagrams for the studied samples are shown in Fig. 4 and the obtained phase shift β as a function of n_e is shown in Fig. 5. The values of β for samples with $n_e = 7.1 \times 10^{17}$ and $2 \times 10^{18} \text{ cm}^{-3}$ were determined from the analysis of SdH oscillations that were reported in [40]. As seen in Fig 5, there is a pronounced abrupt change in β from $\approx \frac{1}{2}$ to ≈ 0 within a narrow concentration interval near $n_e \approx 2 \times 10^{18} \text{ cm}^{-3}$, indicating the drop in Φ_B from $\approx \pi$ to ≈ 0 . We consider such behaviour of Φ_B to be the manifestation of the topological LT in HgSe at critical concentration $n_{LT} \cong 2 \times 10^{18} \text{ cm}^{-3}$. A similar drop in the phase shift of quantum oscillations near the LT point was recently predicted theoretically in 3D topological semimetals in [39]. It is essential that the flattening of $\mu_H(n_e)$ (Region II in Fig.3) occurs below approximately the same electron density n_{LT} as was mentioned above. Here it is important to note that, in contradistinction to the TaAs family of WSMs [34], only the W1-type of Weyl cones is supposed in HgSe [4]. Therefore, the phase shift analysis of SdH oscillations in HgSe is greatly simplified due to the absence of additional modes. The wave vector k_{LT} for the LT is evaluated as $(2F_{LT}e/\hbar)^{\frac{1}{2}} \approx 0.04 \text{ \AA}^{-1}$ where F_{LT} is a SdH oscillation frequency for the sample with $n_e = 2 \times 10^{18} \text{ cm}^{-3}$. This makes it possible to evaluate the key parameter for HgSe as a WSM candidate – the distance between the Weyl nodes Δk_W . Assuming that the separate Fermi spheres of the two Weyl nodes meet at $k_F \approx k_{LT}$, we evaluate $\Delta k_W \cong$

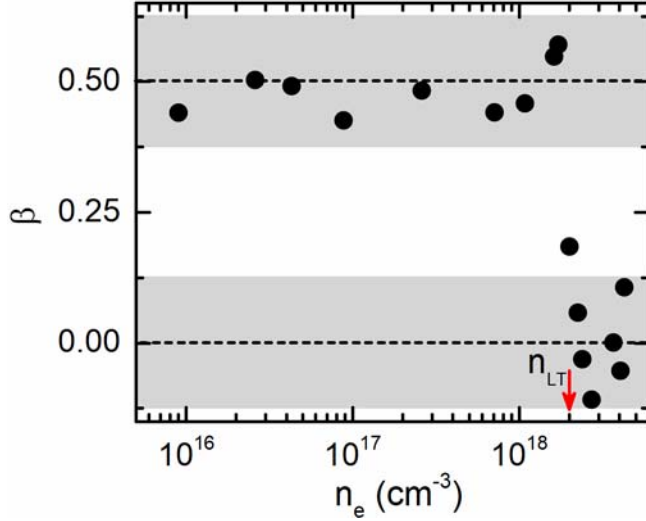


Fig. 5. Phase shift β of SdH oscillations in HgSe as a function of n_e . A pronounced abrupt change in β from $\approx \frac{1}{2}$ to ≈ 0 is seen in the vicinity of the concentration $n_{LT} = 2 \times 10^{18} \text{ cm}^{-3}$ denoted by the arrow. Upper grey area corresponds to non-trivial Berry phase within δ and the lower one to the trivial Berry phase.

$2k_{LT} \approx 0.08 \text{ \AA}^{-1}$. This value is much smaller than the size of the first Brillouin zone in HgSe ($\sim 1 \text{ \AA}^{-1}$) and is well consistent with Δk_W for the TaAs family of WSMs directly measured with ARPES [41]. Thus, the Berry phase may be considered as an appropriate parameter for detection of the LT in WSMs, which occurs by tuning the Fermi level via doping.

In conclusion, we have demonstrated that studies of the effective mass, electron mobility and phase shift of SdH oscillations in HgSe complement each other. Effective mass as a band spectrum parameter points to a deviation of the dispersion relation $\varepsilon(k)$, given by (1), from an ideal linear dispersion at low energy. In contrast to the case of surface states of topological insulators [14], this deviation seems to be unsubstantial and does not shift the Berry phase from π . The non-trivial Berry phase indicates the existence of band touching points in HgSe such as Weyl nodes and related Weyl cones with linear dispersion. The main result is the discovery of the abrupt change $\approx \pi$ of the Berry phase (Fig. 5), which we associate with the LT in HgSe that occurs by tuning the Fermi energy via doping. It is a convincing argument for a topological semimetal phase in HgSe and is consistent with the results of our previous magnetotransport study of HgSe with low electron concentration [4] – non-centrosymmetric WSM candidate.

Acknowledgments. The work was performed as a part of the state task subject “Electron”, S.r.№ AAAA-A18-118020190098-5 and the project №18-10-2-6 of the UB RAS Program with support by the RFBR (Project No. 18-32-00198).

References

1. S. Jia, S.-Y. Xu, and M. Z. Hasan, *Nat. Materials*, **15**, 1140 (2016).
2. M. Z. Hasan, S.-Y. Xu, I. Belopolski, and S.-M. Huang, *Annu. Rev. Condens. Matter Phys.*, **8**, 289 (2017).
3. X. Wan, A. M. Turner, A. Vishwanath, and S. Y. Savrasov, *Phys. Rev. B*, **83**, 205101 (2011).
4. A. T. Lonchakov, S. B. Bobin, V. V. Deryushkin, V. I. Okulov, T. E. Govorkova, and V. N. Neverov, *Appl. Phys. Lett.*, **112**, 082101 (2018).
5. K.-U. Gawlik, L. Kipp, M. Skibowski, N. Orłowski, and R. Manzke, *Phys. Rev. Lett.*, **78**, 16, 3165 (1997).
6. T. Ojanen, *Phys. Rev. B*, **87**, 245112 (2013).
7. J. Ruan1, S.-K. Jian, H. Yao, H. Zhang, S.-C. Zhang, and D. Xing, *Nat. Comm.*, **7**, 11136 (2016).
8. C. R. Whitsett, D. A. Nelson, J.G. Broerman, and E. C. Paxhia, *Phys. Rev. B*, **7**, 10, 4625 (1973).
9. S. L. Lehoczky, J. G. Broerman, D. A. Nelson, and C. R. Whitsett, *Phys. Rev. B*, **9**, 4, 1598 (1974).
10. A. Lenard, M. Arciszewska, T. Dietl, M. Sawicki, W. Plesiewicz, T. Skośkiewicz, W. Dobrowolski, and K. Dybko, *Physica B*, **165&166**, 219 (1990).
11. C. R. Whitsett, *Phys. Rev.*, **138**, 3A, A829 (1965).
12. A. I. Ponomarev, G. A. Potapov, T. I. Kharus, I. M. Tsidilkovski, *Fiz. Tek. Poluprov.*, **13**, 854 (1979) [*Sov. Phys. Semicond.*, **13**, 502 (1979)].
13. I. M. Tsidilkovski, *Springer Series in Solid State Sciences* (Springer, Berlin, New York, 1996), Vol. 116.
14. A. A. Taskin and Y. Ando, *Phys. Rev. B*, **84**, 035301 (2011).
15. A. A. Taskin, Z. Ren, S. Sasaki, K. Segawa, and Y. Ando, *Phys. Rev. Lett.*, **107**, 016801 (2011).
16. E. O. Kane, *J. Phys. Chem. Solids*, **1**, 249 (1957).
17. D. G. Seiler, R. R. Galazka and W. M. Becker, *Phys. Rev. B*, **3**, 12, 4274 (1971).
18. T. Dietl and W. Szymanska, *J. Phys. Chem. Solids*, **39**, 1041 (1978).
19. N. G. Gluzman, A. I. Ponomarev, G. A. Potapov, L. D. Sabirzyanova, I. M. Tsidil'kovskii, *Fiz. Tek. Poluprov.*, **12**, 468 (1978) [*Sov. Phys. Semicond.*, **12**, 271 (1978)].
20. I. M. Lifshitz, *Zh. Eksp. Teor. Fiz.*, **38**, 1569 (1960) [*Sov. Phys. JETP*, **11**, 1130 (1960)].

21. C.-C. Lee, S.-Y. Xu, S.-M. Huang, D. S. Sanchez, I. Belopolski, G. Chang, G. Bian, N. Alidoust, H. Zheng, M. Neupane, B. Wang, A. Bansil, M. Z. Hasan, and H. Lin, *Phys. Rev. B*, **92**, 235104 (2015).
22. N. Xu, G. Autès, C. E. Matt, B. Q. Lv, M. Y. Yao, F. Bisti, V. N. Strocov, D. Gawryluk, E. Pomjakushina, K. Conder, N. C. Plumb, M. Radovic, T. Qian, O. V. Yazyev, J. Mesot, H. Ding, and M. Shi1, *Phys. Rev. Lett.*, **118**, 106406 (2017).
23. C.-L. Zhang, Z. Yuan, Q.-D. Jiang, B. Tong, C. Zhang, X. C. Xie, and S. Jia, *Phys. Rev. B*, **95**, 085202 (2017).
24. T. Liang, Q. Gibson, M. N. Ali, M. Liu, R. J. Cava and N. P. Ong, *Nat. Materials*, **14**, 280 (2015).
25. Y. Zhang, Y.-W. Tan, H. L. Stormer, and P. Kim, *Nat. Lett.*, **438**, 10, 201 (2005).
26. G. P. Mikitik and Yu. V. Sharlai, *Phys. Rev. Lett.*, **82**, 10, 2147 (1999).
27. A. R. Wright and R. H. McKenzie, *Phys. Rev. B*, **87**, 085411 (2013).
28. D. Shoenberg, *Magnetic Oscillations in Metals* (Cambridge University Press, 1984).
29. D.-X. Qu, Y. S. Hor, J. Xiong, R. J. Cava, N. P. Ong, *Science*, **329**, 821 (2010).
30. L. He, F. Xiu, X. Yu, M. Teague, W. Jiang,† Y. Fan, X. Kou, M. Lang, Y. Wang, G. Huang, N.-C. Yeh, and K. L. Wang, *Nano. Lett.*, **12**, 1486 (2012).
31. A. A. Taskin, S. Sasaki, K. Segawa, and Y. Ando, *Phys. Rev. Lett.*, **109**, 066803 (2012).
32. L. P. He, X. C. Hong, J. K. Dong, J. Pan, Z. Zhang, J. Zhang, and S. Y. Li, *Phys. Rev. Lett.*, **113**, 246402 (2014).
33. A. Narayanan, M. D. Watson, S. F. Blake, N. Bruyant, L. Drigo, Y. L. Chen, D. Prabhakaran, B. Yan, C. Felser, T. Kong, P. C. Canfield, and A. I. Coldea, *Phys. Rev. Lett.*, **114**, 117201 (2015).
34. J. Hu, J. Y. Liu, D. Graf, S. M. A. Radmanesh, D. J. Adams, A. Chuang, Y. Wang, I. Chiorescu, J. Wei, L. Spinu & Z. Q. Mao, *Scientific Reports*, **6**, 18674 (2016).
35. B. K. Ridley, *Quantum Processes in Semiconductors* (Oxford University Press, Fifth Edition, UK, 2013).
36. I. A. Luk'yanchuk, and Y. Kopelevich, *Phys. Rev. Lett.*, **93**, 16, 166402 (2004).
37. H. Murakawa, M. S. Bahramy, M. Tokunaga, Y. Kohama, C. Bell, Y. Kaneko, N. Nagaosa, H. Y. Hwang, and Y. Tokura, *Science*, **342**, 1490 (2013).
38. I. M. Tsidilkovski, *International Series on the Science of the Solid State*, **V.19**, Pergamon Press (1982).
39. C. M. Wang, H.-Z. Lu, and S.-Q. Shen, *Phys. Rev. Lett.*, **117**, 077201 (2016).
40. A. I. Ponomarev, G. A. Potapov, I. M. Tsidil'kovskii, *Fiz. Tek. Poluprov.*, **11**, 45 (1977) [Sov. Phys. Semicond. **11**, 24 (1977)].

41. Z. K. Liu, L. X. Yang, Y. Sun, T. Zhang, H. Peng, H. F. Yang, C. Chen, Y. Zhang, Y. F. Guo, D. Prabhakaran, M. Schmidt, Z. Hussain, S.-K. Mo, C. Felser, B. Yan, and Y. L. Chen, *Nat. Materials*, **15**, 27 (2016).